V European Conference on Computational Fluid Dynamics
ECCOMAS CFD 2010
J. C. F. Pereira and A. Sequeira (Eds)
Lisbon, Portugal,14-17 June 2010

ON THE COUPLING OF MICRO AND MESOSCOPIC MODELS IN HEMODYNAMICS

G. Amati*, A.M. Gambaruto†, G. Pontrelli†† and S. Succi††

*CASPUR
Via dei Tizii 6, Roma, Italy
e-mail: G.Amati@caspur.it

†CEMAT-IST
Av. Rovisco Pais 1, Lisbon, Portugal
e-mail: agambar@math.ist.utl.pt

††IAC-CNR
Via dei Taurini 19, Roma, Italy
e-mail: g.pontrelli, s.succi@iac.cnr.it

Key words: Computational fluid dynamics, Lattice Boltzmann methods, moving particle semi-implicit method, multiscale models.

Abstract. *A multiscale procedure to couple a mesoscale Lattice Boltzmann model (LBM) and a microscale particle solver (MPS) for incompressible fluid flows is outlined. While LBM method solves the fluid dynamics in the whole domain, MPS should be used only in selected regions of complex flow field, typically near walls, where a finer scale is required. Preliminary simulations of lid-driven cavity flows at moderate Reynolds numbers show that the MPS is indeed capable of reproducing the main feature of the fluid flow at about ten times the cost of LBM. This permits to estimate the relative size of the high-accuracy regions to be handled by MPS in future multiscale applications to blood flow rheology.*

To assess the solution accuracy of the multiscale approach, the simulation in a driven cavity flow has been carried out as a benchmark. The results of some preliminary numerical tests provide some insights on the capabilities offered by the method in blood flow problems.

1 INTRODUCTION

Computational fluid dynamics has achieved remarkable success for the simulation of industrial and biological flows. In some cases, a variety of interacting scales are present, and a unifying, comprehensive methodology for the whole phenomena remains to be developed. It is hard to simultaneously simulate microlevel scales like droplets and macrolevel free at bulk fluid, because the mesh size used in computational fluid dynamics limit the minimum scale of the simulations. The behaviour of flow field are generally simulated with the Eulerian method or with kinetic methods at mesoscopic level (LBM) over a Cartesian grid.

On the other hand, a number of Lagrangian methods, using particles as grid-free degrees of freedom have been devised [1, 2, 3]. In [4], moving particle semi-implicit (MPS) method was developed to analyze incompressible flows. The governing equations of continuum fluid mechanics are transformed to interactions among particles. The particles then move according to a fully Lagrangian description in the advection step, thus permitting to describe flows with strong contrasts and deformations without resorting to over-demanding grid resolution. The advection equations are explicitly solved, while the Poisson's equation for pressure is implicitly solved. Particle methods are often defined as grid-free methods, making them an attractive alternative to mesh-based methods for flows past complex and deforming boundaries. However, the adaptivity provided by the Lagrangian description can introduce errors and particle methods have often to be coupled with a grid, in order to provide consistent, efficient, and more accurate simulations. Most continuum flows, such as flows in porous media and unsteady separated and turbulent flows, are inherently multiscale, due to the range of scales that govern the underlying physical phenomena. A consistent and systematic framework is necessary to couple microscale and macroscale modelling because the macroscale flows determine the external conditions that influence the microsystem, which in turn influences the larger scales by modifying its boundary conditions [5]. Hybrid methods involve combinations of mesh-based schemes and particle methods in an effort to combine computational advantages of each method. Bridging these two scales in modelling fluid flows offers a tool to efficiently solve problems for which a detailed description of flow is needed in the local regions only, while a plain LBM is employed in the large fluid domain domain [6].

In this paper, we propose a coupled approach which may prove particularly effective for modelling complex flows requiring a detailed insight into specific local regions, such as the case of blood flow in a large artery. Continuum methods are applicable for modelling global arterial dynamics, but are inadequate for the determination of local flows which involve microstructure dynamics. By using a discrete particle method in a small domain, each constituent can be modelled by a microscopic particle within the blood. In the present work, the feasibility of such a coupling is explored by solving the driven cavity flow test case: the critical areas of recirculations and regions of maximum shear need a greater detail and can benefit of the finer description given by the MPS method.

2 FLUID FLOW MODELS AT DIFFERENT SCALES

A variety of methods is available for solving fluid dynamical problems, at different space and time scales. A unifying methodology capable of resolving multiple scales is still missing, whereas a coupling between different computational techniques is an affordable task. Let us first remind here the fundamental principles of two popular methods largely used for a wide class of flow problems.

Lattice-Boltzmann Method

The lattice Boltzmann Method (LBM) has attracted considerable research attention and has emerged as an alternative solution technique to the conventional computational fluid dynamics methods employing Navier-Stokes equations. It offers various advantages, including use of Cartesian grids, high space-time resolution, full scalability on parallel computers, as well as efficient and robust implementation in complex geometries [7].

In LBM, the fluid domain is discretized in uniform Cartesian cells (lattices). Each cell holds a fixed number of density distribution functions, which represent the number of fluid particles moving in these discrete direction. The differential form of the Lattice Boltzmann equation is:

$$\partial_t f_i + \boldsymbol{c}_i \cdot \nabla f_i = -(f_i - f_i^{eq})/\tau \tag{1}$$

where the phase space is discretized into a finite number of particles states i. The variable $f_i(\mathbf{x}, t) \equiv f(\mathbf{x}, \boldsymbol{v} = \boldsymbol{c}_i, t)$ represents the probability of finding a particle at site $\boldsymbol{x}$, at time t and moving along the lattice direction defined by the discrete speed $\boldsymbol{c}_i$. The right hand side of the above equation is the BGK collision operator, which represents particles interaction via a single-time relaxation towards local equilibrium f_i^{eq} on a single timescale τ, called relaxation time [8]. The kinematic viscosity of LBM scheme is proportional to the relaxation time: $\nu = c_s^2(\tau - \frac{\Delta t}{2})$, with a integration scheme having time step Δt. If the fluid is in thermal equilibrium, the distribution is given by the Maxwell-Boltzmann distribution expanded in Taylor series of the fluid speed up to second order:

$$f_i^{eq} = \rho\sigma_i[1 + \beta u_i + \frac{1}{2}(\beta^2 u_i^2 - \beta u^2)] \tag{2}$$

where $\beta = 1/c_s^2$, being c_s the lattice sound speed, ρ the fluid density, $\boldsymbol{u}$ the fluid speed and σ_i the associated weight coefficients. By a Chapman-Enskog analysis, the LBM is proved to approximate the Navier Stokes Equations close to the incompressibility limit. The fluid macroscopic variables are calculated as mass density $\rho = \sum_i f_i$, velocity $\boldsymbol{u} = \sum_i \boldsymbol{c}_i f_i/\rho$ and pressure $p = \rho c_s^2$. In order to recover the correct fluid dynamic equations in the macroscopic limit, the discretization of the velocity space must be performed in such a way to conserve mass, momentum and energy, as well as rotational symmetry. In this work the nine-speed model (known as D2Q9) is used [7]:

$$\boldsymbol{c}_0 = (0, 0), \qquad \boldsymbol{c}_1 = (1, 0), \qquad \boldsymbol{c}_2 = (0, 1)$$

$$\boldsymbol{c}_3 = (-1, 0), \quad \boldsymbol{c}_4 = (0, -1), \quad \boldsymbol{c}_5 = (1, 1)$$
$$\boldsymbol{c}_6 = (-1, 1), \quad \boldsymbol{c}_7 = (-1, -1), \quad \boldsymbol{c}_8 = (1, -1)$$

with weights $\sigma_0 = 4/9$, $\sigma_{1-4} = 1/9$, $\sigma_{5-8} = 1/36$ in eqn. (2).

The method possesses certain clear advantages over conventional CFD method, but the constancy of particle speeds in space results into a spatial uniform Cartesian spatial grid. This represents a very severe limitation for many practical applications, particularly for multiscale type of calculations, where selective distribution of the computational degrees of freedom in the "hot" regions is necessary.

Moving Particle Semi-Implicit Method

Fluid-particle interaction problems can be found in many scientific and engineering applications, such as particle suspensions, lubricated transport, sedimentation, fluvial erosion, and geomechanical systems. The fundamental physical phenomena involved in these problems are generally not well understood and are often described in an empirical fashion, mainly due to the complexity of the fluid-particle interactions. The motion of the particles is driven collectively by the hydrodynamic forces exerted by the fluid, and may also be altered by the interaction between particles. On the other hand, the fluid flow pattern can be strongly affected by the presence of the particles. The numerical method used in this study is the moving particle semi-implicit scheme (MPS), which describes the particle motions and their interactions and is fully based on the Lagrangian description [4]. The key common feature of all particle methods involves the approximation of the Lagrangian form of the Navier-Stokes equations by replacing the derivative operators through equivalent integral operators, that are in turn discretized in terms of particle positions.

Let us consider N particles equidistributed in a 2D domain A. They are approximated by equal spheres having the same mass m and labelled by a subscript capital letter. The particle dynamics is local, being their interactions restricted to within a finite region of influence of radius r_e, through a weighting function (kernel):

$$w(r) = \begin{cases} \dfrac{r_e}{r} - 1 & 0 < r < r_e \\ \\ 0 & r_e < r \end{cases} \tag{3}$$

($r_e = 2.1 \times$ the average initial spacing is typically chosen [4]). This kernel function is used to compute density, repulsive forces, and derivatives as follows. The particle number density at position P is given by:

$$n_P = \sum_{Q \neq P}^{N} w(r_{PQ}) \tag{4}$$

where $r_{PQ} = ||\boldsymbol{x}_P - \boldsymbol{x}_Q||$. For incompressible flows this number should be constant n^0 for all particles. The relation of the particle number density with the actual density is given

by:

$$\rho_P = \frac{m \cdot n_P}{\int\limits_A w(r_{PQ}) dA} \tag{5}$$

The gradient of a quantity ϕ is written as:

$$(\nabla\phi)_P = \frac{d}{n^0} \sum_{Q \neq P} w(r_{PQ}) \frac{(\phi_Q - \phi_P)(\mathbf{x}_Q - \mathbf{x}_P)}{|\mathbf{x}_Q - \mathbf{x}_P|^2} \tag{6}$$

where d is the number of space dimensions (here $d = 2$) [4]. Higher order derivatives are poorly modelled, and the concept of diffusion is used instead:

$$(\nabla^2\phi)_P = \frac{2d}{\lambda n^0} \sum_{Q \neq P} w(r_{PQ})(\phi_Q - \phi_P) \tag{7}$$

with

$$\lambda = \frac{\sum\limits_{Q \neq P} w(r_{PQ}) r_{PQ}^2}{\sum\limits_{Q \neq P} w(r_{PQ})}$$

Meshes are not needed, at any step of the calculation. MPS solves the momentum and the continuity equations:

$$\begin{aligned} \frac{\partial \mathbf{u}}{\partial t} &= -\frac{\nabla P}{\rho} + \nu \nabla^2 \mathbf{u} \\ \frac{1}{\rho}\frac{\partial \rho}{\partial t} &+ \nabla \cdot \mathbf{u} = 0 \end{aligned} \tag{8}$$

as a predictor-corrector method [3, 4]. The corrector step is stabilised by relaxing the incompressibility condition. This is achieved by increasing the diagonal terms of the linear system of a small percentage (typically $1\% - 10\%$). This also speeds up the iterative method (CG) used for its solution.

The time step should be appropriately selected to satisfy the solution accuracy requirement and more importantly to ensure numerical stability due to the explicit nature of the MPS algorithm [1]. The CFL condition $|\mathbf{u}|_{max}\Delta t/\Delta l < 1$ is imposed adaptively, where $|\mathbf{u}|_{max}$ is the maximum particle velocity and Δl is the minimum spacing of particles. Here an upper bound of 0.1 is chosen for the CFL condition, and $\Delta t = (0.1\Delta l)/|\mathbf{u}|_{max}$.

3 COMBINING LBM AND MPS METHODS

In a coupled framework, the fluid field is solved by LBM in the overall domain, while in selected regions particle dynamics is modelled by the MPS. An overlapping stripe separates the two regions and serves to exchange information at the two scale levels.

From micro to mesoscale

Let us consider the average of the density, velocity, ecc. of M particles around a lattice node $G \equiv (j\Delta x, k\Delta x)$, with velocity $\boldsymbol{u}_P$ and position $P = (x_P, y_P)$. The particle contribution to the grid density, momentum and pressure tensor, reads as follows:

$$\begin{aligned}
\rho(G) &= \frac{\sum\limits_P \rho_P W_{PG}}{M} \\
\rho\boldsymbol{u}(G) &= \frac{\sum\limits_P \rho_P W_{PG} \boldsymbol{u}_P}{M} \\
\Pi(G) \equiv \rho\boldsymbol{u}\boldsymbol{u} + p\boldsymbol{I} + \boldsymbol{S} &= \frac{\sum\limits_P \rho_P W_{PG} \boldsymbol{u}_P \boldsymbol{u}_P}{M}
\end{aligned} \tag{9}$$

where $\boldsymbol{S}$ is the dissipative component of the pressure tensor, resulting from gradients of the flow velocity and density. Note this component can be extracted directly from Π since the fluid velocity and density are known independently through the first and second relations above.

In the above

$$\rho_P = \begin{cases} 1 & \text{for} \quad x_j - \dfrac{1}{2} \le x_P \le x_j + \dfrac{1}{2} \quad \text{and} \quad y_k - \dfrac{1}{2} \le y_P \le y_k + \dfrac{1}{2} \\ 0 & \text{otherwise} \end{cases}$$

selects particles lying within a square control volume Ω (see dashed line in fig. 1) and W_{PG} is a suitable particle-to-grid interpolator. Other choices for this control volume are possible. From $\rho(G)$ and $\boldsymbol{u}(G)$, we obtain the equilibrium populations f_i^{eq} at any grid point G:

$$f_i^{eq} = \rho\sigma_i \left\{ 1 + \frac{(\mathbf{c}_i \cdot \mathbf{u})}{c_s^2} + \frac{1}{2c_s^4} u_\alpha u_\beta (c_{i\alpha} c_{i\beta} - c_s^2 \delta_{\alpha\beta}) \right\} \tag{10}$$

where the dependence on G has been omitted for notational simplicity. The above expression corresponds to local kinetic equilibrium, and does not take into account dissipative effects, as expressed by the non-equilibrium component of the distribution function.

The non-equilibrium term is obtained by adding the following second order term in the curly brackets of eqn. (10):

$$f_i^{neq} = \rho\sigma_i \left\{ \frac{1}{2c_s^4} S_{\alpha,\beta}(c_{i\alpha}c_{i\beta} - c_s^2\delta_{\alpha\beta}) \right\} \tag{11}$$

$S_{\alpha,\beta}$ is the shear stress and the sum is also taken over the control volume. This terms includes weak departure from local equilibrium, as dictated by gradients of the density and velocity of the fluid flow. By definition, these departures do not contribute to mass and momentum, since these quantities are conserved by the mesoscopic dynamics, being:

$$\sum_i f_i^{neq} = 0 \qquad \text{and} \qquad \sum_i f_i^{neq} c_\alpha = 0 \tag{12}$$

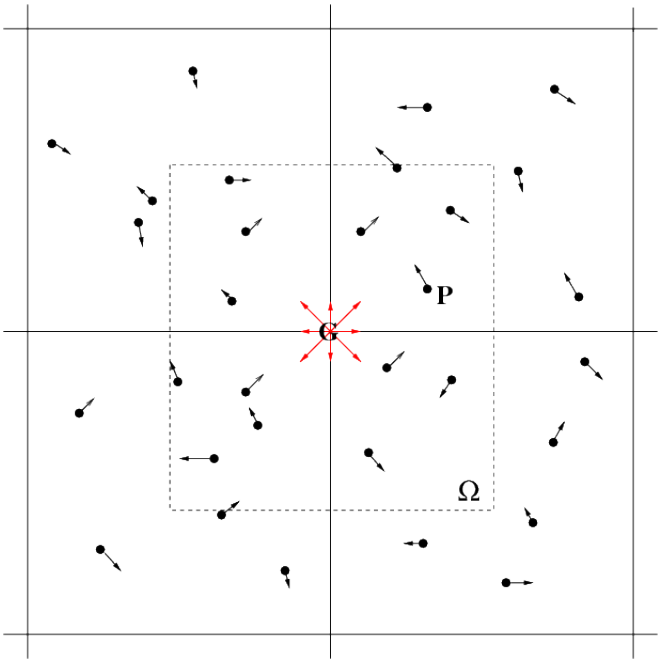

Figure 1: A lattice node $G \equiv (j\Delta x, k\Delta x)$ surrounded by a square control volume Ω (dashed line) with particles P randomly distributed.

From meso to microscale

The transfer from the grid-based mesoscopic distribution function $f_i(G;t)$ to the particle degrees of freedom $\{r_P, \boldsymbol{u}_P\}$ proceeds through a (relatively) standard Monte Carlo sampling procedure [9]. Given the density $\rho(G)$, a set of $N(G) = \rho(G)/(mA)$ particles of mass m are distributed at random positions in the cell of area A, centered about the grid-point G (fig. 1). The particle velocities can then be sampled as follows

$$\boldsymbol{u}_P = \boldsymbol{u}(G) + \boldsymbol{\xi} + \eta(P - G) \cdot \boldsymbol{S}(G) \tag{13}$$

where $\boldsymbol{\xi}$ and η are random quantities with the following properties:

$$< \boldsymbol{\xi} >= 0, \quad < \boldsymbol{\xi} \cdot \boldsymbol{\xi} >= kT/m, \quad < \eta >= 0, \quad (< \eta^2 >)^{1/2} = l_m/l_{PG}, \quad < \boldsymbol{\xi}\eta >= 0$$

Here, l_m is the particle mean-free path, $l_{PG} = ||P - G||$ and $\boldsymbol{S}$ the shear-stress tensor. Clearly, $\boldsymbol{\xi}$ codes for thermal fluctuations at local equilibrium, while η is in charge of gradient-driven departures from local equilibrium (dissipative effects).

4 TOWARDS A MULTISCALE HEMODYNAMICS

The physiological application provides the main source of inspiration of the present work. The principal multiscale aspect of hemodynamics is represented by the cardiovascular network, whose geometrical size ranges from that of large vessels (some mm's diameter) to capillaries (few μm's). The large vessels are the most important elements from a patho-physiological perspective and substantial efforts have been devoted to their accurate modelling with various techniques [10]. Large vessels hemodynamics, as part of a multiscale network, should be coupled with a system of elements, of varying complexity, capable of reproducing the appropriate interaction between the different scales, while guaranteeing at the same time a consistent modelling of the large scale circulatory process [11]. Advanced multiscale methods addressing these network-like aspects of cardiovascular dynamics have been developed in the recent years [11, 12]. While above a certain scale ($\approx 1mm$), blood can be treated as a continuum, it is well known that on a microscopic scale, blood consists of a suspension of corpuscular elements, floating in a liquid plasma [13]. Within the continuum picture, the corpuscular composition of blood is usually accounted for by introducing a non-linear (non-Newtonian) constitutive law between stress and strain. In such a framework, blood presents a shear-dependent viscosity, that increases at low values of the shear rate (shear-thinning behaviour), up to a solid-like behaviour at very small values of the strain-rate (yield stress) [14]. Blood flowing in larger arteries is then described by the Navier-Stokes equations, i.e through a set of continuum fields, such as density, velocity and so on. However, near the wall or in smaller vessels, the granular nature of blood, in fact a collection of red cells of about 8 μm in size, platelets and complex molecules dispersed in the plasma, becomes essential for the quantitative description of complex physico-chemical processes involved in blood cells interactions with endothelial cells, as well as with the microscopic roughness of prosthetic elements [15]. In other words, if current hemodynamics is able to explain, control, or predict circulatory physiological processes that are dominated by mechanical effects (pressure distribution, vortex formation, flow limitation in collapsible tubes, wall elasticity, etc.), there is a larger number of hemodynamical problems, involving the corpuscular nature of the blood and its interaction with the boundaries, that command a microscopic representation, in order to capture hemodynamical phenomena in their entirety. It is therefore extremely desirable to design a new generation of multiscale procedures capable of dealing with blood as a fluid and a particulate at a time.

4.1 Numerical results

The driven cavity flow is chosen as representative of a class of complex problems, including recirculation in saccular aneurysms, present in several blood flow problems. The flow in a 50×50 cavity is induced by a horizontal motion of the upper wall. The Reynolds number, based on the size of the cavity and the velocity of the upper wall, is set to 20. Velocities and pressure given by the advection part of MPS were rearranged with those obtained by the streaming step of LBM.

The velocity patterns obtained by both methods are displayed in fig. 2, from which it is seen that the primary vortex is well captured by MPS. Despite of its preliminary nature, this test bodes well for future concurrent coupling of LBM and MPS aimed at multiscale simulation of complex flows at moderate Reynolds numbers.

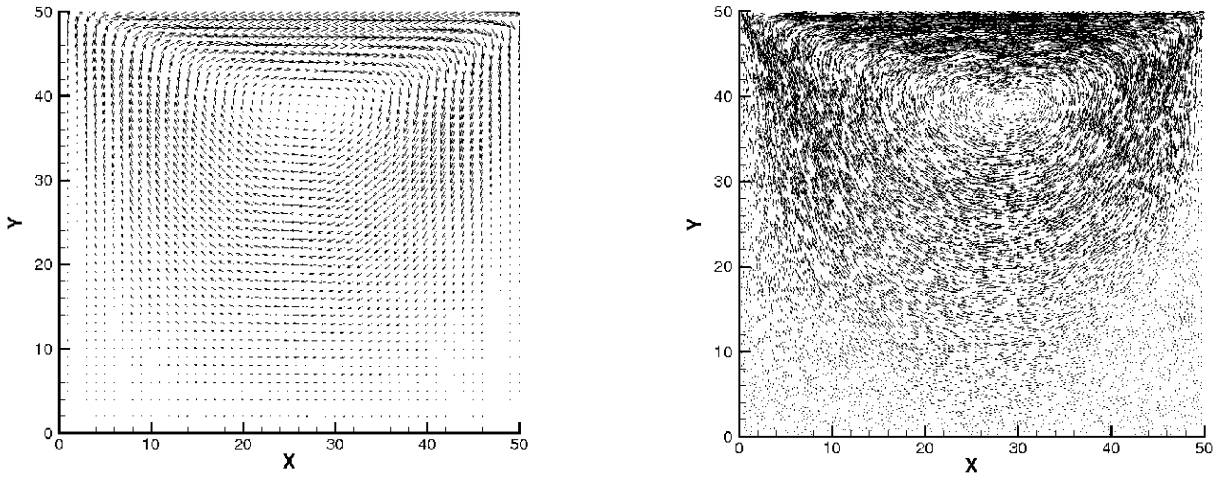

Figure 2: Flow field in the a 50×50 driven cavity steady test problem with Re=20. The comparison shows a LB simulation with 50×50 lattices (left) vs. a MPS simulation having 150×150 particles (right). A suitable coupling of the two methods will enhance the accuracy in the critical regions.

5 CONCLUSIONS

A hybrid method that combines the LBM and MPS methods at different scales is proposed. While the LBM has been well established for mesoscopic flows, at a lower scale the framework of the LBM remains a challenge. Typically, particle methods are used when characteristic length scale is smaller than grid sizes and are mainly used to resolve boundary layers or vortices in critical regions near the wall where the fluid profiles are very sharp. Thus, the multiscale approach is worth to be applied for modelling dilute mixture flow, where a detailed analysis of particle motions is desirable only in small local regions. In such a framework, this paper attempts to indicate a possible coupled strategy for hemodynamical problems that possess intrinsic multiple scales. A worked example as a driven cavity 2D flow illustrates the applicability and the effectiveness of such an

approach. Extension to three-dimensional flows in other complex geometries stands out as a major topic for future research. Work along this direction is currently in progress.

REFERENCES

[1] M. Sueyoshi, M. Kashiwagi, S. Naito, Numerical simulations of wave-induced nonlinear motions of two-dimensional floating body by the moving particle semi-implicit method, *J. Mar. Sci. Technol.*, **13**, 85-94 (2008).

[2] R. M. Nestor, M. Basa, M. Lastiwka, N.J. Quinlan, Extension of the finite volume particle methods to viscous flow, *J. Comp. Physics*, **228**, 1733-1749 (2009).

[3] P. Koumoutsakos, Multiscale flow simulation using particles, *Ann. Rev. Fluid Mech.*, **37**, 457-487 (2005).

[4] S. Koshizuka, A. Nobe, Y. Oka, Numerical analysis of breaking waves using the moving particle semi-implicit method, *Int. J. Num. Meth. Fluids*, **26**, 751-769 (1998).

[5] E. Ishii, T. Ishikawa, Y. Tanabe, Hybrid particle/grid method for predicting motion of micro- and macrofree surfaces, *J. Fluids Eng.*, **128**, 921-930 (2006).

[6] M. Kojic, N. Filipovic, A. Tsuda, A mesoscopic bridging scale method for fluids and coupling dissipative particle dynamics with continuum finite element method, *Comp. Meth. Appl. Mech. Eng.*, **197**, 821-833 (2008).

[7] R. Benzi, S. Succi, M. Vergassola, The lattice Boltzmann equation: theory and applications, *Phys. Rep.*, **222**, 145 (1992).

[8] S. Succi, The lattice Boltzmann equation for fluid dynamics and beyond, Oxford Univ. Press (2001).

[9] F.J. Alexander, A.L. Garcia, The direct simulation Monte Carlo method, *Computers in Physics*, **11**, 588-593 (1997).

[10] L. Formaggia, A. Quarteroni, A. Veneziani (Eds.), Cardiovascular Mathematics: Modeling and simulation of the circulatory system Series: MS&A, **Vol. I** (2009).

[11] R. Ouared, B. Chopard, Lattice Boltzmann Simulations of Blood Flow: Non-Newtonian Rheology and Clotting Processes, *J. Stat. Phys.*, **121**, n. 1-2, 209-221 (2005).

[12] A.G. Hoekstra, J. van't Hoff, A.M. Artoli, P.M.A. Sloot, Unsteady flow in a 2D elastic tube with the LBGK method, *Future Generation Computer Systems*, **20** 6, 917-924 (2004).

[13] A. M. Robertson, A. Sequeira and M. Kameneva, Chapt.: Blood Rheology, in: Hemodynamical Flows: Modeling, Analysis and Simulation,*Oberwolfach Seminars, vol. 37, G.P. Galdi, R. Rannacher, A.M. Robertson and S. Turek, Birkhauswer*, (2008).

[14] A. Artoli, A. Sequeira and J. Janela, Shear-thinning effects in bifurcating blood vessels, *J. Biomech.*, **39**, S310 (2006).

[15] A.M. Artoli, A.G. Hoekstra, P.M.A. Sloot, Mesoscopic simulations of flow in the human abdominal aorta, *J. Biomech.*, **39**, 5, 873-884 (2006).